A Novel Model Predictive Control for Single-Phase Grid-Connected Photovoltaic Inverters

Esmaeil Zangeneh Bighash and
Seyed Mohammad Sadeghzadeh
Faculty of Engineering
Shahed University
Tehran, Iran
Esmaeilzangane@gmail.com and Sadeghzadeh@shahed.ac.ir

Esmaeil Ebrahimzadeh, Yongheng Yang
and Frede Blaabjerg
Department of Energy Technology
Aalborg University
Aalborg, Denmark
ebb@et.aau.dk, yoy@et.aau.dk and fbl@et.aau.dk

***Abstract*- Single-phase grid-connected inverters with LCL filter are widely used to connect photovoltaic systems to the utility grid. Among the existing control schemes, predictive control methods are faster and more accurate but also more complicated to implement. Recently, the Model Predictive Control (MPC) algorithm for single-phase inverter has been presented, where the algorithm implementation is straightforward. In the MPC approach, all switching states are considered in each switching period to achieve the control objectives. However, since the number of switching states in single-phase inverters is small, the inverter output current has a high Total Harmonic Distortions (THD). In order to reduce this, this paper presents an improved MPC for single-phase grid-connected inverters. In the proposed approach, the switching algorithm is changed and the number of the switching states is increased by means of virtual vectors. Simulation results show that the proposed approach lead to a lower THD in the injected current combined with fast dynamics. The proposed predictive control has been simulated and implemented on a 1 kW single-phase HERIC (highly efficient and reliable inverter concept) inverter with an LCL filter at the output.**

Keyword- Model Predictive Control (MPC); Photovoltaic (PV); Total Harmonic Distortion (THD); Highly Efficient and Reliable Inverter Concept (HERIC).

I. INTRODUCTION

Nowadays, the installation of grid-connected single-phase PV inverters has remarkably grown [1], [2]. The most important part of these inverters is the control part. Different control methods for these inverters have been proposed. Linear and non-linear controllers such as hysteresis controller, Proportional Resonant (PR) controllers, Voltage Oriented Control (VOC) controller, sliding mode controller, and also artificial intelligence controllers.

Hysteretic control is simple and robust but has current ripples due to the variable switching frequency [3], [4]. The proportional integral (PI) controller has a long history in control of the power converters, but the PI controller has a steady state error in tracking sinusoidal references [5], [6]. To overcome the problems of conventional PI controllers in the stationary reference frame, the PR controller has been proposed. PR controllers are widely used in the control of single-phase inverters [7], [8], [9]. Other controllers, such as neural networks, sliding mode and fuzzy control methods have high computational burden [10]-[13] and thereby which cost for implementation.

Predictive controllers are easy to implement in digital control system and have fast dynamics, robustness, and low harmonics when system parameters have been properly determined. In order to force the output to track the reference current, these controllers determine the best amount of the inverter voltages [14], [15].

Different predictive control methods based on the deadbeat control have been recently presented to improve the dynamics and the robustness. Some of these methods are the Robust Predictive Current Control (RPCC) [16], the Adaptive Robust Predictive Current Control (ARPCC) [17], the Synchronous Reference Frame Robust Predictive Current Control (SRF-RPCC) [18], the Generalized Robust Predictive Current Control (GRPCC) [19], and Full State Observer Predictive Current Control (FSOPCC) [20]. Although the aforementioned methods have desirable results, high complexity in their calculations become the major drawback. Recently, with the advancement of digital signal processor, the MPC is used to control the power converters. In an MPC approach, the system including inverter, filter and grid is modeled and the next sample of the current is calculated and predicted. Then, the predicted current is compared with the reference current. Consequently, the best switching state can be determined by a cost function [21]-[23].

In [24] and [25] the algorithms based on an MPC control with different control objectives have been presented. However, since the number of switching modes is very small, the accuracy of the method is compromised. Thus, it leads to a high THD in the inverter output current.

In light of the above, this paper presents an improved MPC scheme for a single phase inverter, where the THD of the injected current is improved. In the proposed MPC, the number of switching states have been optimized and increased.

In the proposed MPC, the best switching mode is firstly determined by a cost function. Then the switching time-intervals are calculated and finally, the Space Vector Modulation (SVM) is applied. Simulations have been performed on a 1-kW HERIC inverter system. The results

show that the proposed controller is fast, robust, and accurate and presents a lower THD of the injected current than the traditional MPC.

The rest of this paper is organized as follows: the inverter topology is discussed in section II. Then, the principle of MPC algorithm and the proposed MPC are illustrated. Finally, before the simulation results the proposed MPC is explained in section V.

II. SYSTEM DESCRIPTION

Transformerless inverters that can achieve high efficiency and low cost are widely used in grid-connected PV generation systems. Various transformerless inverter topologies have been proposed to meet the safety requirement of leakage currents, like the VDE-4105 standard [26].

On the other hand, considering the many benefits of LCL filters compared with an L filter, these filter have been extensively used at the output of single-phase PV inverters.

In this paper, one of the single-phase grid-connected transformerless inverters, which has low leakage currents and high efficiency has been used, which is the HERIC inverter with an LCL filter as shown in Fig. 1.

III. PRINCIPLE OF MPC

Model predictive control design and implementation consist of the following three steps:

1- Using a model to predict the behavior of control variables for the next time step.

2- Determining a cost function which includes control objectives and expected behavior of the system.

3- Extract the appropriate command to minimize the cost function value.

The discrete model to predict the next step can be shown in the following equations [22]

$$x(k+1) = Ax(k) + Bu(k)$$
$$y(k) = Cx(k) + Du(k) \quad (1)$$

where $x(k)$ is the current value of the state space variables, $x(k+1)$ is the next value of state space variables, $u(k)$ is the current value of the input variables and $y(k)$ is the current values of the output variables. In the next step, according to the following equation, the cost function can been obtained.

$$J = f(x(k), u(k), \ldots, u(k+N)) \quad (2)$$

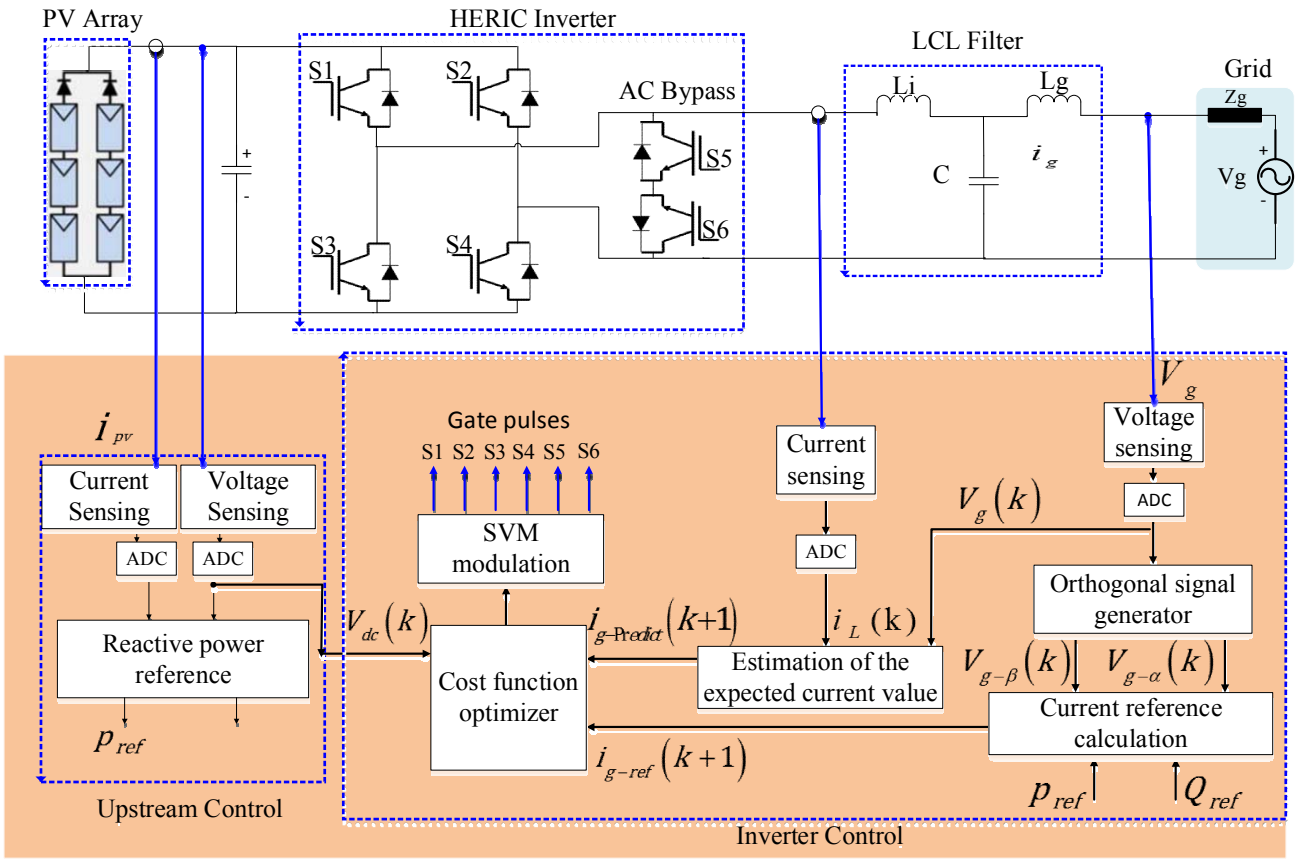

Fig.1. Single-phase HERIC inverter and the proposed MPC.

IV. SYSTEM MODELING

The inverter in Fig. 1 can be described by

$$V_{inv}(\mathrm{t}) = \mathrm{L}_i \frac{di_L(\mathrm{t})}{dt} + V_c(\mathrm{t}) \tag{3}$$

where

$$V_c(\mathrm{t}) = \mathrm{L}_g \frac{di_g(\mathrm{t})}{dt} + V_g(\mathrm{t}) \tag{4}$$

Substituting (4) into (3) gives

$$V_{inv}(\mathrm{t}) = \mathrm{L}_i \frac{di_L(\mathrm{t})}{dt} + \mathrm{L}_g \frac{di_g(\mathrm{t})}{dt} + V_g(\mathrm{t}) \tag{5}$$

$V_{inv}(\mathrm{k})$ is obtained using the Euler equation as

$$V_{inv}(\mathrm{k}) = \mathrm{L}_i \frac{i_L(\mathrm{k+1}) - i_L(\mathrm{k})}{T_S} + \mathrm{L}_g \frac{i_g(\mathrm{k+1}) - i_g(\mathrm{k})}{T_S} + V_g(\mathrm{k}) \tag{6}$$

According to the approximation of the LCL with L filter in [17], $i_g[k] \cong i_L[k]$ and $i_g[k+1] \cong i_L[k+1]$, the predicted current can be obtained as

$$i_{g\_\mathrm{Predict}}(\mathrm{k+1}) = i_g(\mathrm{k+1}) = \frac{T_S}{(\mathrm{L}_i + \mathrm{L}_g)} \times \left(\mathrm{V}_{inv}(\mathrm{k}) - V_g(\mathrm{k})\right) + i_g(\mathrm{k}) \tag{7}$$

the cost function in the proposed method can be written as

$$g = \left| i_{g\_ref}(\mathrm{k+1}) - i_{g\_\mathrm{Predict}}(\mathrm{k+1}) \right| \tag{8}$$

where $i_{g\_ref}(\mathrm{k+1})$ can be obtained from the active and reactive power reference and orthogonal signals of the grid as

$$i_{g\_\mathrm{ref}}(\mathrm{k+1}) = \frac{2}{v_{g\alpha}(\mathrm{k+1})^2 + v_{g\beta}(\mathrm{k+1})^2} * \begin{bmatrix} V_{g\alpha}(\mathrm{k+1}) & V_{g\beta}(\mathrm{k+1}) \end{bmatrix} \begin{bmatrix} P_{ref} \\ Q_{ref} \end{bmatrix} \tag{9}$$

in (12), $V_{g\alpha}(k+1)$ and $V_{g\beta}(k+1)$ are orthogonal signals of $V_g(k+1)$ with $V_g(k+1)$ being calculated by

$$v_g(\mathrm{k+1}) = \left| V_g \right| \sin(\omega(\mathrm{k}) + \Delta\varphi) \tag{10}$$

in which $\omega(k)$ is the frequency of the grid voltage detected by the PLL in the k[th] sample, $|V_g|$ is the peak of the grid voltage and $\Delta\varphi$ is the phase between two samples determined by

$$\Delta\varphi = \frac{2\pi}{(\mathrm{f}_{sw} / \mathrm{f}_{grid})} \tag{11}$$

where f_{sw} and f_{grid} are the switching frequency and the grid frequency, respectively.

V. THE PROPOSED MPC

Fig. 2 shows the switching states in the single-phase HERIC inverter.

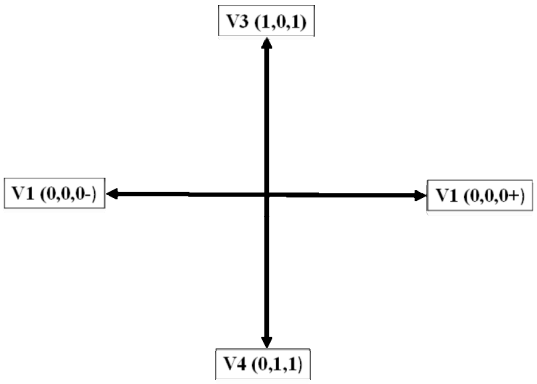

Fig. 2. Voltage vectors generated by the HERIC inverter.

According to Fig. 2, space vector switching states in the HERIC inverter can been shown as a function of S_a, S_b and S_c:

$$S_a = \begin{cases} 1, & S_1 = 1 \,\&\, S_3 = 0 \\ 0, & S_0 = 0 \,\&\, S_3 = 1 \end{cases} \tag{12}$$

$$S_b = \begin{cases} 1, & S_2 = 1 \,\&\, S_4 = 0 \\ 0, & S_2 = 0 \,\&\, S_4 = 1 \end{cases} \tag{13}$$

$$S_c = \begin{cases} 1, & S_5 = 0 \,\&\, S_6 = 0 \\ 0^+, & S_5 = 0 \,\&\, S_6 = 1 \\ 0^-, & S_5 = 1 \,\&\, S_6 = 0 \end{cases} \tag{14}$$

The definition of S_c is different with S_a and S_b. State 0^+ means the zero state before the positive half cycle and State 0^- means the zero state before the negative half cycle. The HERIC inverter switching space vector can be given as

$$S = (\mathrm{S}_a + \mathrm{aS}_b)\mathrm{S}_c \tag{15}$$

where $a = e^{j\pi}$ and finally the inverter output voltage is defined as

$$V_o = SV_{dc} \tag{16}$$

as seen in Fig. 2, the number of states is small, which makes the inverter output voltage inaccurate. It leads to harmonics in the injected current to the network because the large state between 0 to $+V_{dc}$ and 0 to $-V_{dc}$ are ignored. In the conventional MPC, this cause a poor performance in terms of THD. Therefore, this paper presents an improved MPC, which applies multiple switching vectors. Fig. 3 shows all the vectors in the proposed MPC.

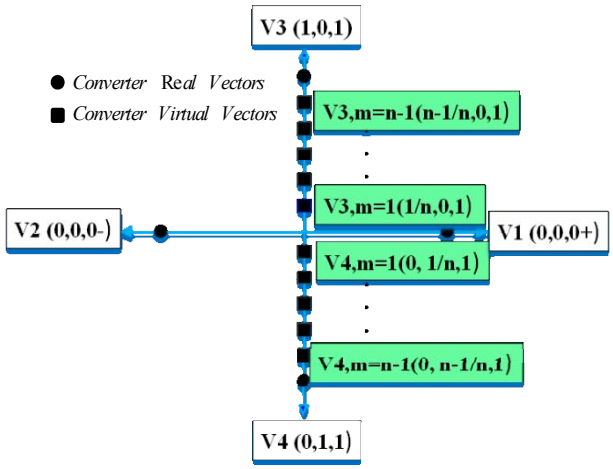

Fig. 3. Voltage vectors for the HERIC inverter with virtual vectors.

These vectors include four basic or real vectors (the circle symbols in Fig. 3) and several virtual vectors (the square symbols in Fig. 3). The virtual vectors have been selected as optimized states. In fact, the virtual vectors are generated with a combination of the basic vectors. The duration of these vectors will be a fraction of the switching cycle and during the rest time of the switching cycle zero vectors will be applied. For example, when a basic vector, $V_3(1,0,1)$ or $V_4(0,1,1)$, is selected, this vector will be applied in the entire cycle switching. When a virtual vector, $V_3(m/n,0,1)$ or $V_4(0,m/n,1)$, is selected at first, the basic vector, $V_3(1,0,1)$ or $V_4(0,1,1)$,will be applied for m/n% of switching cycle and then for the rest of time (T_0) $V_1(0,0,0^+)$ or $V_2(0,0,0^-)$ will be applied.

In the proposed MPC control, the inverter voltage can be obtained as

$$V_{inv} = \frac{m}{n} V_{dc} \tag{17}$$

All the states of V_{inv} in (17), where m varies from 1 to the specified value n, will be placed in (7) and $i_{g\_Predict}(k+1)$ can be calculated. Then, $i_{g\_Predict}(k+1)$ is obtained by minimizing the cost function. The amount of V_{inv} that minimizes the cost function is the inverter voltage reference V_{inv}^* and will determine T_d or the duty cycle as

$$T_d = \frac{V_{inv}^*}{V_{dc}} T_S \text{, or, } T_d = \frac{m}{n} T_S \tag{18}$$

where T_s is the switching period. Following, V_{inv}^* vector is applied during T_d and then the zero vector should be applied in the period of T_0 time. In this case,

$$T_0 = T_S - T_d \tag{19}$$

according to HERIC inverter characteristics, depending on T_d that has been in positive or negative cycle during the time period of T_0 time, $V_1(0,0,0^+)$ or $V_2(0,0,0^-)$ will be applied.

VI. Simulation Results

Simulations have been done in MATLAB using PLECS blocks. In the beginning, the controller sets the current reference $i_{g\_ref}(k+1)$ based on the reference of the active and reactive power specified from the upstream control, i.e., according to (12). Then, the reference is compared with the estimated current value in (10) and eventually, the proposed MPC will make the final decision to determine the switching modes (by employing a cost function). Fig. 1 shows a closed loop system for the single-phase PV inverter. It can be seen in Fig. 1 that at the first stage of the control blocks, one Orthogonal Signal Generator (OSG) is needed. In this paper an OSG algorithm has been selected [27].

Two simulations have been done. In the first simulation, the amount of the active power is set to 1 kW and the reactive power reference is set to zero.

In order to validate the effectiveness of the proposed method, several modes are studied. In each mode, the number of vectors will change. For example, in the first case, the number of switching vectors is 4 as the traditional MPC in Fig. 2 (two zero modes, one positive mode and one negative mode). In the second case, the number of switching vectors is 12 (2 zero modes, 5 positive modes and 5 negative modes). For the third case, 32 vectors (2 zero modes, 15 positive modes and 15 negative modes). In the last case 82 vectors (2 zero modes, 40 positive modes and 40 negative modes) is used.

Fig. 4 shows the results of the HERIC inverter with different vectors. As it is seen in Fig. 4, the THD of the injected current is strongly reduced when the number of vectors increases.

Another simulation has been done to test the dynamic response and the robustness of the proposed controller. In this case, the active and reactive power references are changed, where the reference of the reactive power changes from 0 to 700 Var and the reference of the active power changes from 1000 to 400 W. Finally, the power references will restore to the original states. Simulation results are shown in Fig. 5.

As it is seen in Fig. 5, the inverter can quickly follow the references, which shows that the proposed MPC control is precise and robust.

Also, a short circuit operation has been studied and a reference current of 5 A is given to be tracked by the proposed controller. The results of this case are shown in Fig. 6. As it is shown in Fig. 6, the proposed controller in the short circuit time is robust and can track the reference current.

Finally, control block diagrams of the proposed MPC is shown in Fig.7.

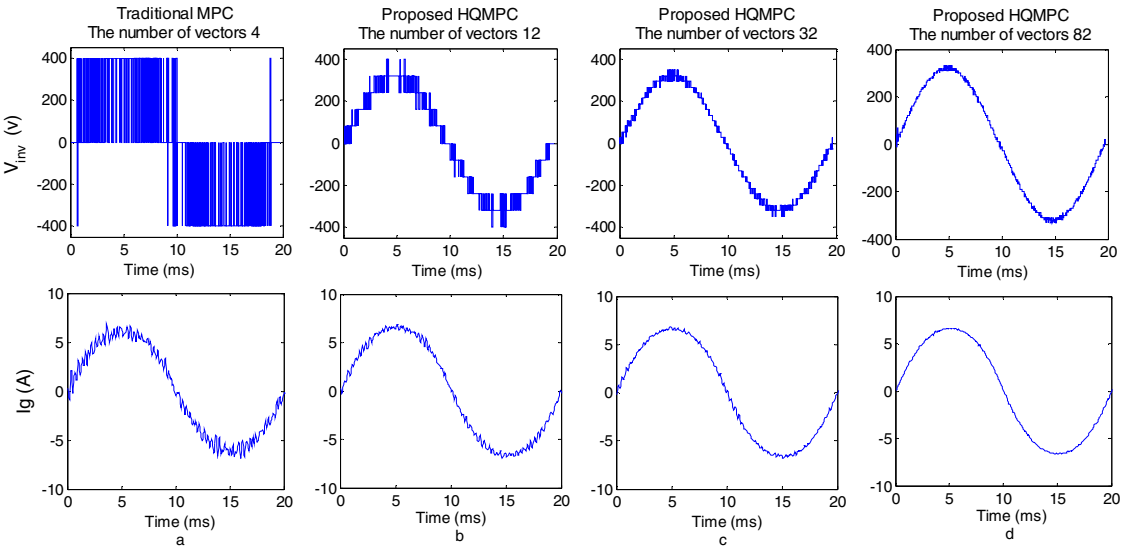

Fig. 4. The avarage of inverter voltage (top) and grid current (bottom) in four case, (a) 4 vectors, (b) 12 vectors, (c) 32 vectors and (d) 82 vectors.

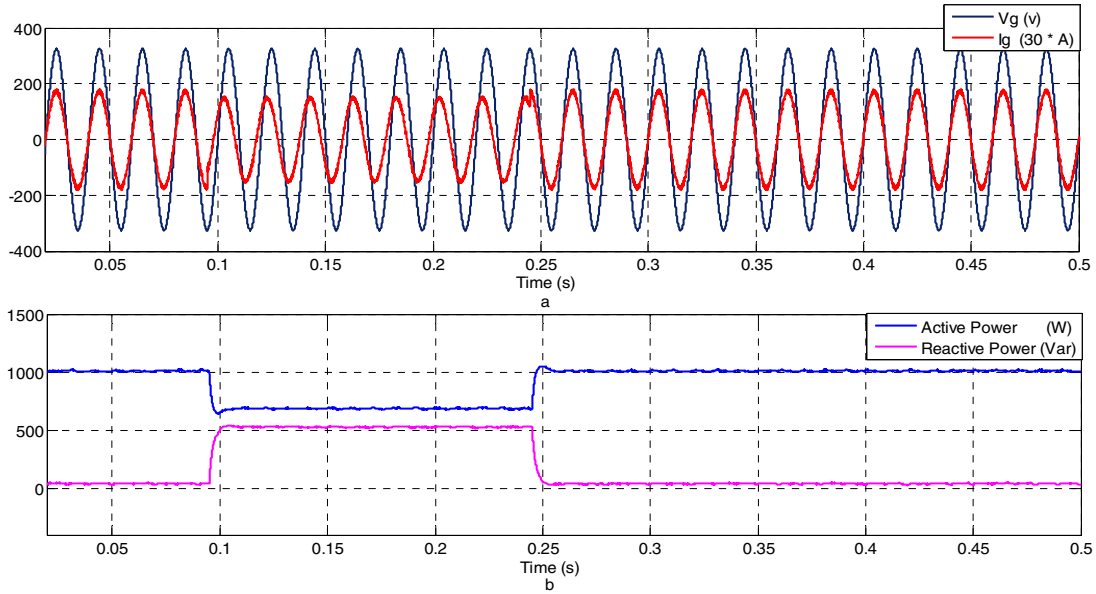

Fig.5. Performance of the grid-connected transformerless HERIC inverter with the proposed controller: (a) grid voltage $\boldsymbol{V_g}$(volts) and grid current $\boldsymbol{i_g}$(30 * A), (b) active power (W) and reactive power (Var) b.

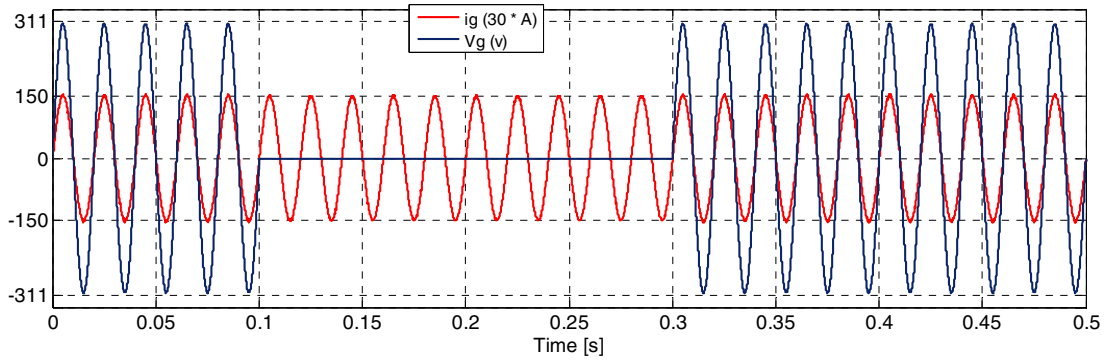

Fig. 6. Grid voltage (V_g) and current (i_g) in the case of a short-circuit operation with the proposed controller.

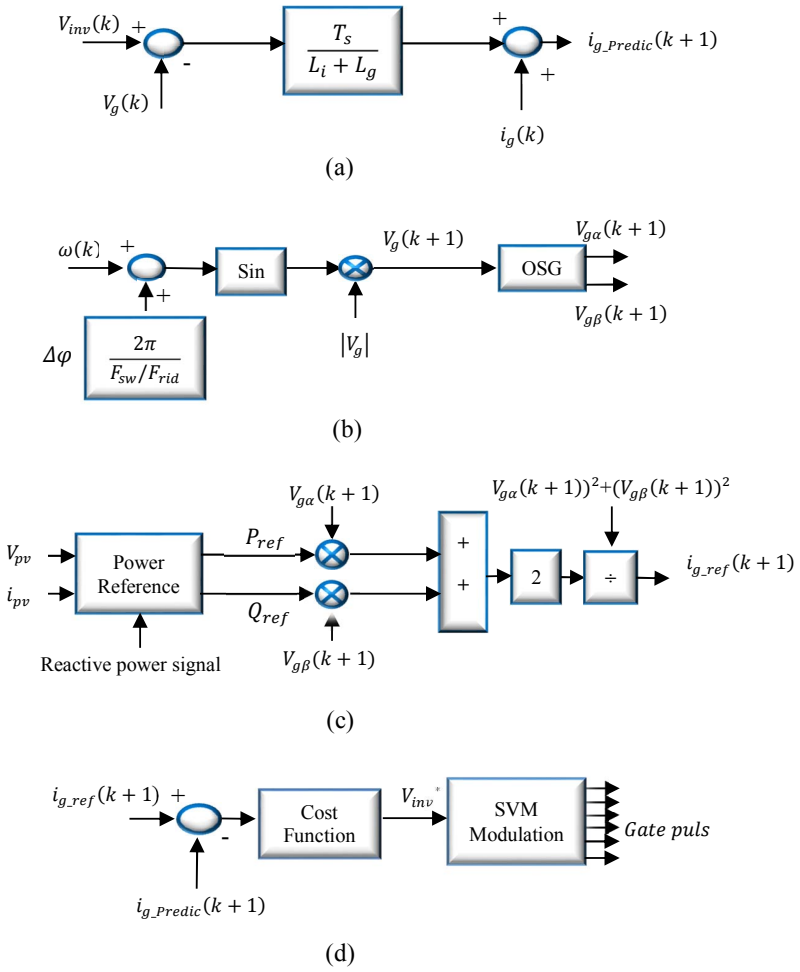

Fig. 7. Control block diagram of the proposed MPC.

VII. Conclusion

In this paper, a new model predictive method has been presented for a HERIC inverter, where simplicity and lack of gain tuning have been achieved. The proposed method is easy compared the prior-art robust predictive control methods. Simulation results have demonstrated that this method has high accuracy, fast response, good robustness and high quality in term of injected current to network. It can be applied in to the control of the single-phase inverters without much computational burden but achieving a high quality.

References

[1] "Global market outlook for photovoltaics 2014-2018," [Online]. Available: http://resources.solarbusinesshub.com.

[2] "Global market outlook for solar power 2015-2019," [Online]. Available: http://resources.solarbusinesshub.com.

[3] A. B. Plunkett, "A current controlled PWM transistor inverted drive," *in Proc. IEEE IAS Annu. Meet*, 1979, pp. 785–792.

[4] W. Stefanutti and P. Mattavelli, "Fully digital hysteresis modulation with switching-time prediction," *IEEE Trans. Ind. Appl.*, vol. 42, no. 3, pp. 763–769, Jun. 2006.

[5] D. M. Brod and D. W. Novotny, "Current control of VSI-PWM inverters," *IEEE Trans. Ind. Appl.*, vol. IA-21, no. 3, pp. 562-570, May. 1985.

[6] J. Dannehl, C. Wessels and F. W. Fuchs, "Limitations of voltage-oriented PI current control of grid-connected PWM rectifiers with filters*," IEEE Trans. I Ind. Electron.,* vol. 56, no. 2, pp. 380-388, Feb. 2009.

[7] M. Castilla, J. Miret, J. Matas, L. Garcia de Vicuna and J. M. Guerrero, "Control design guidelines for single-phase grid-connected photovoltaic inverters with damped resonant harmonic compensators," *IEEE Trans. Ind. Electron.*, vol. 56, no. 11, pp. 4492-4501, Nov. 2009.

[8] D. N. Zmood, D. G. Holmes, "Stationary frame current regulation of PWM inverters with zero steady-state error," *IEEE Trans. Power Electron.*, Vol. 18, No. 3, May. 2003.

[9] M. Ciobotaru, R. Teodorescu and F. Blaabjerg, "Control of single-stage single-phase PV inverter," in *Proc. EPE*, 2005, pp. 1-10 .

[10] F. J. Lin, K. C. Lu and B. H. Yang, “Recurrent fuzzy cerebellar model articulation neural network based power control of a single-stage three-phase grid-connected photovoltaic system during grid faults,” *IEEE Trans. Ind. Electron*., vol. 64, no. 2, pp. 1258-1268, Feb. 2017.
[11] S. Li, M. Fairbank, C. Johnson, D. C. Wunsch, E. Alonso, and J. L. Proano, “Artificial neural networks for control of a grid-connected rectifier/inverter under disturbance, dynamic and power converter switching conditions,” *IEEE Trans. Neural Netw. Learn. Syst.*, vol. 25, no. 4, pp. 738–750, Apr. 2014.
[12] X. Fu and S. Li, “Control of single-phase grid-connected converters with LCL filters using recurrent neural network and conventional control methods,” *IEEE Trans. Power Electron*., vol. 31, no. 7, pp. 5354-5364, Jul. 2016.
[13] X. Hao, X. Yang, T. Liu, L. Huang, and W. Chen, “A sliding-mode controller with multiresonant sliding surface for single-phase grid-connected VSI with an LCL filter,” *IEEE Trans. Power Electron.*, vol. 28, no. 5, pp. 2259–2268, May. 2013.
[14] P. Wipasuramonton, Z. Q. Zhu, and D. Howe, “Predictive current control with current-error correction for PM brushless AC drives,” *IEEE Trans. Ind. Appl.*, vol. 42, no. 4, pp. 1071–1079, Jul./Aug. 2006.
[15] J. Rodriguez, J. Pontt, C. A. Silva, P. Correa, P. Lezana, P. Cortes, and U. Ammann, “Predictive current control of a voltage source inverter,” *IEEE Trans. Ind. Electron*., vol. 54, no. 1, pp. 495–503, Feb. 2007.
[16] J. C. Moreno, J. M. Espi Huerta, R. G. Gil and S. A. Gonzalez, “A robust predictive current control for three-phase grid-connected inverters,” *IEEE Trans. Ind. Electron.*, vol. 56, no. 6, pp. 1993-2004, Jun. 2009.
[17] J. Espi, J. Castello, R. Garcia-Gil, G. Garcera, and E. Figueres, “Aadaptive robust predictive current control for three-phase grid-connected inverters,” *IEEE Trans. Ind. Electron.*, vol. 58, no. 8, pp. 3537–3546, Aug. 2011.
[18] J. M. Espi Huerta, J. Castello, J. R. Fischer, and R. Garcia-Gil, “A synchronous reference frame robust predictive current control for threephase grid-connected inverters,” *IEEE Trans. Ind. Electron.*, vol. 57, no. 3, pp. 954 – 962, Mar. 2010.
[19] J. Castello, J. M. Espí and R. Garcia-Gil, “A new generalized robust predictive current control for grid-connected inverters compensates anti-aliasing filters delay,” *IEEE Trans. Ind. Electron.*, vol. 63, no. 7, pp. 4485-4494, Jul. 2016.
[20] J. Fischer, S. Gonzalez, M. Herran, M. Judewicz, and D. Carrica, “Calculation-delay tolerant predictive current controller for three-phaseinverters,” *IEEE Trans. Ind. Informat.*, vol. 10, no. 1, pp. 233–242, Feb. 2014.
[21] P. Cortes, G. Ortiz, J. I. Yuz, “Model predictive control of an inverter with output LC filter for UPS applications, ” *IEEE Trans. Ind. Electron.*, vol. 56, no. 6, pp. 1875–1883, Jun. 2009.
[22] J.Rodriguez and P.Cortes, “Predictive control of the converters and electrical drives” *Wiley, first edition*, 2012, ISBN 978-1-119-96398-1.
[23] H.T. Moon, H.S. Kim, and M.J. Youn, “A discrete-time predictive current control for PMSM,” *IEEE Trans. Power Electron.*, vol. 18, no. 1, pp. 464–472, Jan. 2003.
[24] X. Li, M. B. Shadmand, R. S. Balog and H. A. Rub, “Model predictive decoupled power control for single-phase grid-tied inverter,” *in Proc. PECI*, 2015, pp. 1-7.
[25] Y. Xingwu, J. Hongchao and G. Wei, “Model predictive control of single phase grid-connected inverter,” *in Proc. APPEEC*, 2014, pp. 1-4.
[26] L. Zhang, K. Sun, Y. Xing and M. Xing, “H6 transformerless full-bridge PV grid-tied inverters, ” *IEEE Trans. Power Electron., vol. 29, no. 3, pp. 1229-1238, Mar. 2014.*
[27] J. W. Choi, Y. K. Kim and H. G. Kim, “Digital PLL control for single-phase photovoltaic system," *in Proc. IEE P-Elect Pow Appl.*, 2006, pp. 40-46.